Communication

Dendrimer-inspired nanomaterials for the in vivo delivery of siRNA to lung vasculature

Omar F. Khan, Edmond W. Zaia, Siddharth Jhunjhunwala, Wen Xue, Wenxin Cai, Dong Soo Yun, Carmen Barnes, James E. Dahlman, Yizhou Dong, Jeisa M. Pelet, Matthew J Webber, Jonathan Tsosie, Tyler Jacks, Robert Langer, and Daniel G. Anderson

Nano Lett., **Just Accepted Manuscript** • DOI: 10.1021/nl5048972 • Publication Date (Web): 19 Mar 2015

Dendrimer-inspired nanomaterials for the in vivo delivery of siRNA to lung vasculature

Omar F. Khan,[1] Edmond W. Zaia,[1] Siddharth Jhunjhunwala,[1] Wen Xue,[1,2] Wenxin Cai,[1] Dong Soo Yun,[1] Carmen Barnes,[4] James E. Dahlman,[1,5] Yizhou Dong,[1,3] Jeisa M. Pelet,[1] Matthew J. Webber,[1] Jonathan K. Tsosie,[1] Tyler E. Jacks,[1,2,6] Robert Langer,[1,5,7] Daniel G. Anderson.[1,5,7]*

[1] Koch Institute for Integrative Cancer Research, Massachusetts Institute of Technology, Cambridge, Massachusetts 02139, USA

[2] Howard Hughes Medical Institute, Massachusetts Institute of Technology, Cambridge, Massachusetts 02139, USA

[3] Department of Anesthesiology, Children's Hospital Boston, 300 Longwood Avenue, Boston, MA 02115, USA

[4] Alnylam Pharmaceuticals, Cambridge, MA 02142, USA

[5] Harvard-MIT Division of Health Sciences and Technology, Institute for Medical Engineering and Science, Massachusetts Institute of Technology, Cambridge, Massachusetts 02139, USA

[6] Department of Biology, Massachusetts Institute of Technology, Cambridge, Massachusetts 02139, USA

[7] Department of Chemical Engineering, Massachusetts Institute of Technology, Cambridge, Massachusetts 02139, USA

Abstract

Targeted RNA delivery to lung endothelial cells has potential for treatment for conditions that involve inflammation, such as chronic asthma, and obstructive pulmonary disease. To this end, chemically-modified dendrimer nanomaterials were synthesized and optimized for targeted small interfering RNA (siRNA) delivery to lung vasculature. Using a combinatorial approach, the free amines on multigenerational poly(amido amine) and poly(propylenimine) dendrimers were substituted with alkyl chains of increasing length. The top performing materials from *in vivo* screens were found to primarily target Tie2-expressing lung endothelial cells. At high doses, the dendrimer-lipid derivatives did not cause chronic increases in proinflammatory cytokines, and animals did not suffer weight loss due to toxicity.. We believe these materials have potential as agents for the pulmonary delivery of RNA therapeutics.

Keywords

siRNA, target lung endothelial cells, in vivo, modified dendrimer nanoparticles, nanomaterial

Introduction

Pathologic gene expression in cells can be suppressed through RNA interference (RNAi). RNAi is triggered when small interfering RNA (siRNA) for a specific gene is introduced into

cells, which leads to the degradation of the corresponding mRNA gene transcripts.[1, 2] To enhance the usability of this naturally occurring phenomena for the treatment of lung diseases, new materials must be developed to nanoencapsulate siRNA strands, deliver them to specific lung cell subpopulations and avoid any non-specific or off-target effects. The preferential targeting of lung endothelial cells is especially desirable for injuries and diseases that result in lung vascular inflammation. Examples of such conditions include lung inflammation and reduced function after transplantation,[3] barotrauma caused by the use of external ventilators,[4] and exacerbated pulmonary inflammation in asthmatics and chronic obstructive pulmonary disease (COPD) patients.[5] These conditions can lead to ischemic lung injury. The pulmonary endothelium is an ideal target for therapeutic siRNA delivery because it not only controls vascular permeability,[6] but can also modulate the innate immune response by releasing cytokines and recruiting circulating leukocytes.[7]

The most advanced work in nanomaterial-based siRNA delivery include hepatocyte-specific nanoparticles which have shown both selectivity and potency in non-human primates and clinical trials.[8-13] While more challenging to achieve, there is an increasing collection of reports of siRNA delivery to tissues other than hepatocytes including tumors,[14, 15] immune cells[16] and endothelium.[17] This work reports on the development of formulations based on dendrimeric nanomaterials that have been optimized for lung endothelium delivery. The central hypothesis was that nanoparticles created from symmetric, highly-branched ionizable nanomaterials are capable of preferentially delivering siRNA payloads to the lung endothelium when administered intravenously.

Branched polyethylenimines (PEI), which are ionizable polycations, have been used to successfully deliver siRNA payloads.[18, 19] Randomly branched low molecular weight PEIs

modified with alkyl chains have been developed for siRNA delivery[19] and modifications using ethyl acrylate and succinic acid groups have also shown efficacy, though to a lesser extent.[20] However, while the PEI branching results in increased cationic charge density at low pH, it is not molecularly defined; instead, it is a polydisperse polymer mixture with random branching. In this way, dendrimers are advantageous because of their regulated, step-wise growth and defined branching patterns. While poly(amido amine) and poly(propylenimine) dendrimers have been used in both modified and unmodified forms to deliver siRNA,[21-25] modifications to dendrimers that result in preferential siRNA delivery to lung endothelial cells have not been reported.

Results

The chemically-modified dendrimers were synthesized using Michael addition chemistry by combining poly(amido amine) or poly(propylenimine) dendrimers of increasing generations with alkyl epoxides of various carbon chain length (**Scheme 1**). The products were purified with flash chromatography. The resulting product contained a mixture of different substitutions when examined using thin layer chromatography (R_f between 0.4 and 0.8 for an 87.5:11:1.5 CH_2Cl_2:MeOH:NH_4OH_{aq} solvent system). The dendrimer cores are ionizable and cationic at physiological pH, which makes them ideal for forming complexes with negatively charged siRNA. Initially, the chemically-modified dendrimer nanoparticles were tested *in vitro* for Tie2 gene knockdown in both immortalized and primary endothelial cells. Tie2 was selected as a gene target because it is almost exclusively expressed by endothelial cells.[26-28] In these screens, the only excipient used was 1,2-dimyristoyl-sn-glycero-3-phosphoethanolamine-N-[methoxy(polyethylene glycol)-2000] (1,2-dimyristoyl-sn-glycero-3-phosphoethanolamine-N-

mPEG$_{2000}$). This was done to reduce the formulation complexity. Nanoparticles had a modified dendrimer: Tie2 siRNA mass ratio of 5:1 and a 4:1 molar ratio of modified dendrimer to 1,2-dimyristoyl-sn-glycero-3-phosphoethanolamine-N-mPEG$_{2000}$. The chemically-modified dendrimers that displayed the best performance in primary endothelial cells (**Figure 1a**) were then injected into the tail veins of healthy 8 week old female C57BL/6 mice. After 3 days, mice were sacrificed and mRNA levels were quantified in the harvested tissues (**Figure 1b**). The top 4 candidates from these screens were the generation 1 poly(amido amine) dendrimer with C_{15} lipid tails (PG1.C15), and generation 1 poly(propylenimine) dendrimers with C_{14}, C_{15} and C_{16} lipid tails (DG1.C14, DG1.C15 and DG1.C16, respectively).

Because the modified dendrimer materials contained a mix of dendrimer cores with different levels of free amine alkyl chain substitution, the materials were further fractionated by flash chromatography. This was done to determine which degree of substitution resulted in the highest level of activity. The mixtures were initially divided into two fractions: R_f between 0.4 and 0.6 for less substituted materials and R_f between 0.6 and 0.8 for more substituted materials (87.5:11:1.5 CH_2Cl_2:MeOH:NH_4OH_{aq} solvent system). The *in vivo* performance of the subfractions were compared to that of the mixture in terms of Tie2 knockdown. As seen in **Figure 2a**, the mixture outperformed that of the fractions, implying that a broad range of substitutions had a greater, synergistic effect.

To select the top 3 materials, nanoparticles that readily aggregated were removed from contention. This was done to avoid injecting large nanoparticle aggregates into animals. The propensity for aggregation was gauged by the magnitude of their zeta potential. Of the top 4 candidates, DG1.C16 had the least favorable (i.e. smallest) zeta potential, which predicted aggregation **(Table 1)**. As predicted, aggregation was observed when DG1.C16 particles were

stored at 4°C. The aggregation was likely caused by the longer C_{16} lipid tail, which reduce overall solubility in aqueous environments. DG1.C14 and DG1.C15 both possess shorter lipid chains, and so were more soluble. DG1.C16 was also redundant because the two remaining poly(propylenimine)-based nanoparticles (DG1.C14 and DG1.C15) exhibited the same level of protein knockdown as seen by Western blot **(Figure 2b)**. Supporting Information (SI) Figure S1 shows the NMR spectra of the lead materials.

To improve the efficiency of PG1.C15, DG1.C14 and DG1.C15 nanoparticles, the overall formulation ratios and inclusion of additional excipients, such as cholesterol, were tested *in vivo*. Cholesterol is an important component in the lipid envelope of viruses[29] and has been used in many potent nanoparticle formulations.[8-10, 12] It was discovered that the addition of cholesterol improved *in vivo* Tie2 lung knockdown (**Figure 3a**). Moreover, the addition of cholesterol appeared to alter the mean diameter and polydispersity index of the nanoparticles (**Figure 3b** and **SI Table S2**).

To confirm knockdown was caused by the successful delivery of Tie2 siRNA and not due to the modified dendrimer material itself, animals were treated with optimized modified dendrimer formulations carrying non-functional luciferase siRNA as a control. As expected, these formulations resulted in no Tie2 gene knockdown (**Figure 3c**). Tie2 knockdown was also examined in the endothelium of other organs but was most potent in the lung endothelium (**SI Figure S2**). **Figure 3d** shows the structure of these optimized nanoparticles and their optimized formulation ratios are shown in **Table 2**. Using Tie2 siRNA, a dose response was performed to examine low-dose efficiency (**Figure 4a**). Interestingly, when all three types of nanoparticles were combined in a single dose, Tie2 knockdown in lung endothelial did not surpass the level of

knockdown observed with individual nanoparticles. In terms of uptake mechanism, this may indicate some type of molecular competition or blockage.

To qualitatively gauge the relative differences in lung delivery between the different chemically-modified dendrimers, nanoparticles containing Cy5.5-labelled siRNA were injected into mice and their lung fluorescence imaged after 1 hour (**Figure 4b**). While DG1.C15 appeared to qualitatively show a greater amount of fluorescence, it was unclear if this was due to increased endothelial cell delivery or delivery to other cells types within the lung. To address this question, preferential nanoparticle association with lung endothelial cells was confirmed using flow cytometry (**Figure 5a, 5b** and **SI Figure S3**). As an additional check, Tie2 siRNA was replaced with Itgb1 siRNA (**Figure 5c**). Itgb1, or fibronectin receptor, beta subunit, is more ubiquitous than Tie2. It is an important protein in cell-matrix adhesion,[30] and it is expressed in both the endothelial and epithelial cells of the lung. Thus, if nanoparticles were capable of broader delivery, one would observe a greater amount of Itgb1 knockdown. Here, DG1.C14 and DG1.C15 showed modest knockdown of Itgb1 (37 and 30%, respectively) and no knockdown with PG1.C15. These results appeared to parallel the Cy5.5-labelled siRNA fluorescence data where the lungs from DG1.C14 and DG1.C15 treatments showed more fluorescence than PG1.C15 ones (**Figure 4b**). Hence, the greater amount of relative fluorescence in DG1.C14 and DG1.C15 was attributed to an increased uptake in additional cell types.

Furthermore, as shown in **Figure 5c**, these nanoparticles were ineffective in terms of siRNA delivery to epithelial lung tumors, which were generated by the targeted mutation of Kras and p53 genes in mice (KP mice).[31] In this model, the lung tumor cells primarily expressed $Kras^{G12D}$, and not the endothelial cells. Using this KP mouse lung tumor model, a previously reported low molecular weight polyethyleneimine-based polymer was capable of targeting both

lung endothelial cells and epithelial lung tumor cells.[19, 32] Moreover, previous studies have suggested that tumors experience increased uptake due to the enhanced permeation and retention effect and their leaky vasculature.[33] Thus, to test tumor uptake and gene silencing, KP mice were treated with a high cumulative dose of 4 mg/kg Kras siRNA nanoparticles. Interestingly, no Kras mRNA knockdown was found in the epithelial lung tumors. Thus, because of their narrow targeting, these materials are primarily suitable for targeting lung endothelium and not lung tumor cells.

In addition to effective lung endothelial cell targeting, nanomaterials must not cause chronic increases in proinflammatory cytokines. For example, in the case of human lung transplantation, inflammatory cytokines such as TNF-α, IFN-γ, IL-8, IL-12 and IL-18 are elevated, which can contribute to ischemic injury and diminish long-term graft function.[34] If used to treat lungs post transplantation, the chemically-modified dendrimers must not exacerbate the inflammatory response by causing an increase in these cytokines. As a preliminary screen to determine whether the chemically-modified dendrimers cause a chronic increase in these and other cytokines, plasma cytokine levels were measured 48 hours after high, medium and low doses in mice (**SI Figure S4**). Fortuitously, no statistically significant increases in these and other inflammation-related cytokines were observed. Additionally, no changes in mouse bodyweights were observed when injected with high doses of the nanoparticles (**SI Figure S5**).

Discussion

The nanoencapsulation of siRNA and its successful delivery to lung endothelial cells *in vivo* was achieved through the use of modified poly(amido amine) and poly(propylenimine)

dendrimers substituted with hydrophobic lipid tails. The modification process resulted in a mixture of substitutions. As seen in **Figure 2a**, nanoparticles created from a mixture of substitutions outperformed those that were composed on smaller fractions, which implied that a broad range of substitutions had a greater, synergistic effect. We believe the enhanced potency was caused by changes to the nanoparticles' *in vivo* biomolecular corona,[35] which in turn affected trafficking into the endothelial cells. Nanoparticles formed from a mixture of modified dendrimer molecules may adsorb different types or amounts of serum proteins. For example, nanoparticles coated with serum albumin have shown greater endothelial cell uptake in culture.[36] In a similar way, the optimized formulations that included cholesterol (**Figure 3a)** reduced the overall amount of (1,2-dimyristoyl-sn-glycero-3-phosphoethanolamine-N-mPEG$_{2000}$), which is used to mitigate protein adsorption to the particle. When coupled with the addition of cholesterol, it is likely that more serum proteins were able to adsorb to the nanoparticle, which in turn enhanced endothelial cell uptake.

To improve the potency of gene knockdown in lung endothelial cells, nanoparticle formulations were optimized to include cholesterol, which markedly improved gene knockdown efficiency (**Figure 3a**). However, some knockdown (albeit to a lesser degree) was still observed in other organs at high doses (**SI Figure S2**), which means off-target effects in the endothelial cells of other organs were not completely abolished. To compensate for this, lower doses should be used.

Prior to optimization, DG1.C14 was the most potent nanoparticle. After optimization, the diameters of PG1.C15 and DG1.C15 nanoparticles increased, while DG1.C14 did not **(Figure 3b** and **SI Table S2)**. Interestingly, PG1.C15 and DG1.C15 showed the greatest improvement in

potency. This may indicate that each type of modified dendrimer nanoparticle has a critical diameter for optimal endothelial cell delivery.

Furthermore, the chemical structure of these modified dendrimers are likely to play a role in endothelial cell delivery and potency. The core of the PG1.C15 molecule has amide bonds, which are not present in the DG1.C14 and DG1.C15 materials. These amide bonds may, at least in part, be responsible for the narrower targeting window of PG1.C15 (**Figure 5c**).

Additionally, the apparent nanoparticle pK_a values of these materials are different (**Table 1**). Since apparent nanoparticle pK_a has been shown to influence siRNA nanoparticle efficacy,[37, 38] these differences may also play a role.

Conclusions

In summary, siRNA formulated with chemically-modified dendrimers have shown a high avidity for Tie2-positive endothelial cells in the lung. The PG1.C15, DG1.C14 and DG1.C15 can be used to preferentially target endothelial cells within the lung. We believe these formulations may have utility in the treatment of injuries and diseases that arise from dysfunctional endothelium. Additionally, the use of molecularly defined, regularly-branched, ionizable dendrimers as the core structure for these materials is advantageous with respect to clinical translation. While demonstrated with siRNA here, we expect that these formulations of these materials could have use for the delivery of other therapeutic nucleic acids, such as mRNA, microRNA, and DNA.

Methods

Alkyl epoxides: C_{10}, C_{12}, C_{14} and C_{16} epoxides were purchased from TCI or Sigma. C_{15} epoxide was not commercially available and was synthesized by the dropwise addition of 1-pentadecene (TCI) to a 2x molar excess of 3-chloroperbenzoic acid (Sigma) in dichloromethane (BDH) under constant stirring at room temperature. After reacting for 8 hours, the reaction mixture was washed with equal volumes of super saturated aqueous sodium thiosulfate solution (Sigma) three times. After each wash, the organic layer was collected using a separation funnel. Similarly, the organic layer was then washed three times with 1 M NaOH (Sigma). Anhydrous sodium sulfate was added to the organic phase and stirred overnight to remove any remaining water. The organic layer was concentrated under vacuum to produce a slightly yellow, transparent oily liquid. This liquid was vacuum distilled to produce the clear, colorless C_{15} epoxide liquid.

Modified dendrimer synthesis: Poly(amido amine) or poly(propylenimine) dendrimers of increasing generations (Sigma Aldrich and SyMo-Chem) were reacted with alkyl epoxides of various carbon chain length. The stoichiometric amount of epoxide was equal to the total number of amine reactive sites within the dendrimer (2 sites for primary amines and 1 site for secondary amines). Reactants were combined in cleaned 20 mL amber glass vials. Vials were filled with 200 proof ethanol as the solvent and reacted at 90°C for 48 hours in the dark under constant stirring. The crude product was mounted on a Celite™ 545 (VWR) pre-column and purified via flash chromatography using a CombiFlash Rf machine with a RediSep Gold Resolution silica column (Teledyne Isco) with gradient elution from 100% CH_2Cl_2 to 75:22:3 CH_2Cl_2/MeOH/NH_4OH_{aq} (by volume) over 40 minutes. Thin layer chromatography (TLC) was used to test the eluted fractions for the presence of chemically-modified dendrimers using an

87.5:11:1.5 CH_2Cl_2/MeOH/NH_4OH_{aq} (by volume) solvent system. Chemically-modified dendrimers with different levels of substitution appeared as a distinct band on the TLC plate. The desired fractions were combined, dried under vacuum and stored under a dry, inert atmosphere until used. All products contained a mixture of conformational isomers.

Nanoparticle formulation: Tie2, Itgb1, CD45, luciferase and Alexa Fluor 647-labelled GFP siRNA were supplied by Alnylam Pharmaceuticals and Kras siRNA was purchased from Dharmacon. Because the mice used in these studies did not possess GFP and luciferase genes, these siRNAs were used as a non-functional controls. All siRNA sequences are shown in SI Table S1. Nanoparticles were formulated using a microfluidic mixing device, as described elsewhere[39] using the conditions found in Table 2. The 1,2-dimyristoyl-sn-glycero-3-phosphoethanolamine-N-[methoxy(polyethylene glycol)-2000] excipient was purchased from Avanti Polar Lipids and cholesterol from Sigma. Nanoparticle size and zeta potential were characterized with a Zetasizer NanoZS machine (Malvern). For accurate dilutions and dosage, the concentration of siRNA was determined by a combination of Ribogreen assay (Invitrogen) and NanoDrop measurement (Thermo Scientific). Apparent nanoparticle pK_a was determined as previously described.[39] The specific doses for each experiment are listed in the main body of this manuscript and are given as mg siRNA per kg mouse bodyweight.

In vivo animal experiments: 8-10 week old, female C57BL/6 mice were used in all experiments, with the exception of Kras experiments, where KP mice[31] were used. All procedures used in animal studies conducted at MIT were approved by the Institutional Animal Care and Use Committee (IACUC) and were also consistent with all applicable local, state and federal regulations.

Flow cytometry: Mice were injected with a 2.5 mg siRNA/kg bodyweight dose of Alexa Fluor 647-tagged siRNA nanoparticles though the tail vein. One hour post injection, mice were euthanized and their lungs were perfused with 15 mL of saline. Harvested lungs were minced and digested for 1 hour at 37°C and 750 RPM in a PBS solution (Gibco) containing 0.92 M HEPES (Gibco), 201.3 units/mL collagenase I (Sigma), 566.1 units/mL collagenase XI (Sigma) and 50.3 units/mL DNase I (Sigma). Following digestion, cells and tissue debris were passed through a 70 μm filter using a 1 mL syringe and the digestion buffer washed away by centrifuging the single cell suspension at 400 RCF for 4 minutes at 4°C. Red blood cells in the cell suspension were lysed using the ACK lysis buffer (Life Technologies, USA) and the remaining cells suspended in flow cytometry buffer (PBS containing 0.5% BSA and 2mM EDTA). For antibody staining, approximately 1 million cells were mixed with 100 μl flow cytometry buffer containing anti-mouse CD45 (clone 30-F11), anti-mouse CD31 (clone 390) and anti-mouse EPCAM (clone G8.8) (Biolegend, San Diego, USA). Staining was performed at 4°C for 20 min. Cells were suspended in flow cytometry buffer containing propidium iodide for analysis. Flow cytometry was performed using a BD LSR-II and data analyzed using FlowJo (Treestar Inc., USA). Endothelial cells were gated as CD31+ CD45- EPCAM-, immune cells as CD45+ CD31- EPCAM- and epithelial cells as EPCAM+ CD31- CD45-.

CD45 knockdown: 8-10 week old, female C57BL/6 mice (Charles River) were intravenously injected via the tail vein with CD45 siRNA-carrying nanoparticles at a dose of 1 mg siRNA/kg bodyweight. After 3 days, spleens were harvested, processed and analyzed as described previously.[39]

Quantifying gene silencing: A QuantiGene 2.0 assay was used to quantify gene expression according to a previously published protocol.[39] Kras silencing experiments were

performed in KP mice[40] at a total dose of 4 mg Kras siRNA/kg bodyweight. RT-PCR was used to determine Kras silencing and data analyzed using the $\Delta\Delta C_T$ method.

Protein expression: Western blots were used to determine Tie2 protein expression levels in lungs. Frozen pulverized lung tissue powder was dissolved in RIPA Lysis and Extraction Buffer and Halt Protease and Phosphatase Inhibitor Cocktail (Pierce Biotechnology). Proteins were extracted into the buffer at 4°C while mixing at 1400 RPM. Total protein concentration was determined by the Pierce BCA protein assay kit (Thermo Scientific). Each lane of the pre-cast Mini-PROTEAN TGX 4-15% polyacrylamide gradient gels (Bio-rad) was loaded with equal amounts of total protein. After electrophoresis and transfer to nitrocellulose membrane (Bio-rad), equal total protein loading was confirmed by Ponceau S staining (Sigma). Blots were blocked in Odyssey blocking solution and probed overnight with primary antibodies against Tie2 (R&D Systems) and β-actin (Sigma) followed by incubation in secondary LI-COR antibodies (LI-COR Biosciences). Blots were imaged using a LI-COR Odyssey imaging system.

Cell culture: HMVEC-L were cultured in EGM-2 media (Lonza) and bEnd.3 in Dulbecco's Modified Eagle's Medium supplemented with fetal bovine serum (ATCC). For *in vitro* screening, cells were seeded and grown to confluence in tissue culture treated 96 well plated. Cells were treated with nanoparticles at a 50 nM siRNA dose overnight before lysis and mRNA quantification using the QuantiGene 2.0 Reagent System and QuantiGene 2.0 mRNA probes (Affymetrix). Primary endothelial cells were used below passage 8.

Cytokine screen: Blood samples were collected at 2 days following tail vein injection of modified dendrimer nanoparticles in C57BL/6 mice, and plasma was isolated for cytokine array screening using the Bio-Plex Protein Array System (Bio-Rad) with a Luminex 200 instrument.[39]

The Bio-Plex Pro™ Mouse Cytokine 23-plex panel was combined with the Bio-Plex Pro™ Mouse Cytokine 9-plex panel for an array totaling 32 cytokines.

Statistical analysis: Either ANOVA with the Tukey multiple comparison correction or the student t-test was used to gauge statistically significant differences in mean values. P values less than 0.05 were considered statistically significant. Statistical analysis was performed using version 16 of the SPSS statistics software package.

ASSOCIATED CONTENT

Supporting Information

NMR spectra, organ screen data, immune cell data, blood inflammatory cytokine screen, bodyweight data, siRNA sequences and full ANOVA table from library screen. This material is available free of charge via the Internet at http://pubs.acs.org.

AUTHOR INFORMATION

Corresponding Author

* Correspondence should be addressed to Daniel G. Anderson; e-mail: dgander@mit.edu

Author Contributions

O.F.K., C.B. and J.E.D. conceived the modified dendrimer concept. O.F.K. designed experiments. E.W.Z. assisted with animal experiments. E.W.Z and J.K.T. performed NMR. D.S.Y. conducted high-resolution transmission electron microscopy. W.X. generated KP mice

and W.C. performed the PCR reactions. M.J.W. performed inflammatory cytokine screen. S.J. and J.M.P. assisted with flow cytometry studies. Y.D. provided assistance with material purification. O.F.K. and D.G.A. primarily prepared the manuscript with input from all other authors.

Funding Sources

This work was funded by the National Institutes of Health Centers of Cancer and Nanotechnology Excellence (U54 CA151884), the United States Army Medical Research and Materiel Command's Armed Forces Institute of Regenerative Medicine (W81XWH-08-2-0034) and Alnylam Pharmaceuticals. W.X. was supported by fellowships from the American Association for Cancer Research and the Leukemia Lymphoma Society and is currently supported by grant 1K99CA169512. M.J.W. received support from the Juvenile Diabetes Research Fund. J.E.D. received support from the NDSEG, NSF GRFP, and the MIT Presidential Fellowships.

Notes

R.L. is a shareholder and member of the Scientific Advisory Board of Alnylam. R.L and D.G.A have sponsored research grants from Alnylam.

ACKNOWLEDGMENT

We expresses our gratitude towards J. Robert Dorkin, Hao Yin, Roman L. Bogorad and Kevin J. Kauffman for useful advice and discussions. Tyler E. Jacks is a Howard Hughes Investigator, the David H. Koch Professor of Biology, and a Daniel K. Ludwig Scholar.

Animal experiments were performed at the Massachusetts Institute of Technology's Division of Comparative Medicine. Lung tissue processing and IVIS imaging was performed in the Swanson Biotechnology Center in the Koch Institute for Integrative Cancer Research at the Massachusetts Institute of Technology. We thank the Koch Institute's Nanotechnology Materials Lab for their cryogenic transmission electron microscopy service.

REFERENCES

1. Fire, A.; Xu, S.; Montgomery, M. K.; Kostas, S. A.; Driver, S. E.; Mello, C. C., Potent and specific genetic interference by double-stranded RNA in Caenorhabditis elegans. *Nature* **1998,** *391* (6669), 806-11.
2. Elbashir, S. M.; Lendeckel, W.; Tuschl, T., RNA interference is mediated by 21-and 22-nucleotide RNAs. *Genes Dev.* **2001,** *15* (2), 188-200.
3. Shreeniwas, R.; Schulman, L. L.; Narasimhan, M.; McGregor, C. C.; Marboe, C. C., Adhesion molecules (E-selectin and ICAM-1) in pulmonary allograft rejection. *Chest* **1996,** *110* (5), 1143-1149.
4. Tremblay, L. N.; Slutsky, A. S., Ventilator-induced injury: From barotrauma to biotrauma. *Proc. Assoc. Am. Phys.* **1998,** *110* (6), 482-488.
5. Tao, F.; Gonzalez-Flecha, B.; Kobzik, L., Reactive oxygen species in pulmonary inflammation by ambient particulates. *Free Radic. Biol. Med.* **2003,** *35* (4), 327-340.
6. Dejana, E.; Orsenigo, F.; Lampugnani, M. G., The role of adherens junctions and VE-cadherin in the control of vascular permeability. *J. Cell Sci.* **2008,** *121* (13), 2115-2122.
7. Weber, C.; Fraemohs, L.; Dejana, E., The role of junctional adhesion molecules in vascular inflammation. *Nat. Rev. Immunol.* **2007,** *7* (6), 467-477.
8. Dong, Y.; Love, K. T.; Dorkin, J. R.; Sirirungruang, S.; Zhang, Y.; Chen, D.; Bogorad, R. L.; Yin, H.; Chen, Y.; Vegas, A. J.; Alabi, C. A.; Sahay, G.; Olejnik, K. T.; Wang, W.; Schroeder, A.; Lytton-Jean, A. K.; Siegwart, D. J.; Akinc, A.; Barnes, C.; Barros, S. A.; Carioto, M.; Fitzgerald, K.; Hettinger, J.; Kumar, V.; Novobrantseva, T. I.; Qin, J.; Querbes, W.; Koteliansky, V.; Langer, R.; Anderson, D. G., Lipopeptide nanoparticles for potent and selective siRNA delivery in rodents and nonhuman primates. *Proc. Natl. Acad. Sci. U. S. A.* **2014,** *111* (11), 3955-60.
9. Novobrantseva, T. I.; Borodovsky, A.; Wong, J.; Klebanov, B.; Zafari, M.; Yucius, K.; Querbes, W.; Ge, P.; Ruda, V. M.; Milstein, S.; Speciner, L.; Duncan, R.; Barros, S.; Basha, G.; Cullis, P.; Akinc, A.; Donahoe, J. S.; Jayaprakash, K. N.; Jayaraman, M.; Bogorad, R. L.; Love, K.; Whitehead, K.; Levins, C.; Manoharan, M.; Swirski, F. K.; Weissleder, R.; Langer, R.; Anderson, D. G.; De Fougerolles, A.; Nahrendorf, M.; Koteliansky, V., Systemic RNAi-mediated Gene Silencing in Nonhuman Primate and Rodent Myeloid Cells. *Mol. Ther.--Nucleic Acids* **2012,** *1*.
10. Love, K. T.; Mahon, K. P.; Levins, C. G.; Whitehead, K. A.; Querbes, W.; Dorkin, J. R.; Qin, J.; Cantley, W.; Qin, L. L.; Racie, T.; Frank-Kamenetsky, M.; Yip, K. N.; Alvarez, R.; Sah, D. W.; de Fougerolles, A.; Fitzgerald, K.; Koteliansky, V.; Akinc, A.; Langer, R.; Anderson, D. G., Lipid-like materials for low-dose, in vivo gene silencing. *Proc. Natl. Acad. Sci. U. S. A.* **2010,** *107* (5), 1864-9.

11. Maier, M. A.; Jayaraman, M.; Matsuda, S.; Liu, J.; Barros, S.; Querbes, W.; Tam, Y. K.; Ansell, S. M.; Kumar, V.; Qin, J.; Zhang, X.; Wang, Q.; Panesar, S.; Hutabarat, R.; Carioto, M.; Hettinger, J.; Kandasamy, P.; Butler, D.; Rajeev, K. G.; Pang, B.; Charisse, K.; Fitzgerald, K.; Mui, B. L.; Du, X.; Cullis, P.; Madden, T. D.; Hope, M. J.; Manoharan, M.; Akinc, A., Biodegradable lipids enabling rapidly eliminated lipid nanoparticles for systemic delivery of RNAi therapeutics. *Mol. Ther.* **2013,** *21* (8), 1570-8.
12. Jayaraman, M.; Ansell, S. M.; Mui, B. L.; Tam, Y. K.; Chen, J.; Du, X.; Butler, D.; Eltepu, L.; Matsuda, S.; Narayanannair, J. K.; Rajeev, K. G.; Hafez, I. M.; Akinc, A.; Maier, M. A.; Tracy, M. A.; Cullis, P. R.; Madden, T. D.; Manoharan, M.; Hope, M. J., Maximizing the potency of siRNA lipid nanoparticles for hepatic gene silencing in vivo. *Angew. Chem.* **2012,** *51* (34), 8529-33.
13. Coelho, T.; Adams, D.; Silva, A.; Lozeron, P.; Hawkins, P. N.; Mant, T.; Perez, J.; Chiesa, J.; Warrington, S.; Tranter, E.; Munisamy, M.; Falzone, R.; Harrop, J.; Cehelsky, J.; Bettencourt, B. R.; Geissler, M.; Butler, J. S.; Sehgal, A.; Meyers, R. E.; Chen, Q.; Borland, T.; Hutabarat, R. M.; Clausen, V. A.; Alvarez, R.; Fitzgerald, K.; Gamba-Vitalo, C.; Nochur, S. V.; Vaishnaw, A. K.; Sah, D. W.; Gollob, J. A.; Suhr, O. B., Safety and efficacy of RNAi therapy for transthyretin amyloidosis. *N. Engl. J. Med.* **2013,** *369* (9), 819-29.
14. Davis, M. E.; Zuckerman, J. E.; Choi, C. H. J.; Seligson, D.; Tolcher, A.; Alabi, C. A.; Yen, Y.; Heidel, J. D.; Ribas, A., Evidence of RNAi in humans from systemically administered siRNA via targeted nanoparticles. *Nature* **2010,** *464* (7291), 1067-1070.
15. Park, J. H.; von Maltzahn, G.; Xu, M. J.; Fogal, V.; Kotamraju, V. R.; Ruoslahti, E.; Bhatia, S. N.; Sailor, M. J., Cooperative nanomaterial system to sensitize, target, and treat tumors. *Proc. Natl. Acad. Sci. U. S. A.* **2010,** *107* (3), 981-6.
16. Novobrantseva, T. I.; Borodovsky, A.; Wong, J.; Klebanov, B.; Zafari, M.; Yucius, K.; Querbes, W.; Ge, P.; Ruda, V. M.; Milstein, S.; Speciner, L.; Duncan, R.; Barros, S.; Basha, G.; Cullis, P.; Akinc, A.; Donahoe, J. S.; Jayaprakash, K. N.; Jayaraman, M.; Bogorad, R. L.; Love, K.; Whitehead, K.; Levins, C.; Manoharan, M.; Swirski, F. K.; Weissleder, R.; Langer, R.; Anderson, D. G.; De Fougerolles, A.; Nahrendorf, M.; Kotelianský, V., Systemic RNAi-mediated gene silencing in nonhuman primate and rodent myeloid cells. *Mol. Ther.--Nucleic Acids* **2012,** *1*.
17. Santel, A.; Aleku, M.; Keil, O.; Endruschat, J.; Esche, V.; Durieux, B.; Loffler, K.; Fechtner, M.; Rohl, T.; Fisch, G.; Dames, S.; Arnold, W.; Giese, K.; Klippel, A.; Kaufmann, J., RNA interference in the mouse vascular endothelium by systemic administration of siRNA-lipoplexes for cancer therapy. *Gene Ther.* **2006,** *13* (18), 1360-1370.
18. Grayson, A. C. R.; Doody, A. M.; Putnam, D., Biophysical and structural characterization of polyethylenimine-mediated siRNA delivery in vitro. *Pharm. Res.* **2006,** *23* (8), 1868-1876.
19. Dahlman, J. E.; Barnes, C.; Khan, O. F.; Thiriot, A.; Jhunjunwala, S.; Shaw, T. E.; Xing, Y.; Sager, H. B.; Sahay, G.; Speciner, L.; Bader, A.; Bogorad, R. L.; Yin, H.; Racie, T.; Dong, Y.; Jiang, S.; Seedorf, D.; Dave, A.; Singh Sandhu, K.; Webber, M. J.; Novobrantseva, T.; Ruda, V. M.; Lytton-Jean, A. K.; Levins, C. G.; Kalish, B.; Mudge, D. K.; Perez, M.; Abezgauz, L.; Dutta, P.; Smith, L.; Charisse, K.; Kieran, M. W.; Fitzgerald, K.; Nahrendorf, M.; Danino, D.; Tuder, R. M.; von Andrian, U. H.; Akinc, A.; Panigrahy, D.; Schroeder, A.; Kotelianský, V.; Langer, R.; Anderson, D. G., In vivo endothelial siRNA delivery using polymeric nanoparticles with low molecular weight. *Nat. Nanotechnol.* **2014,** *9* (8), 648-55.
20. Zintchenko, A.; Philipp, A.; Dehshahri, A.; Wagner, E., Simple modifications of branched PEI lead to highly efficient siRNA carriers with low toxicity. *Bioconjugate Chem.* **2008,** *19* (7), 1448-1455.
21. Omidi, Y.; Hollins, A. J.; Drayton, R. M.; Akhtar, S., Polypropylenimine dendrimer-induced gene expression changes: The effect of complexation with DNA, dendrimer generation and cell type. *J. Drug Target.* **2005,** *13* (7), 431-443.
22. Taratula, O.; Savla, R.; He, H. X.; Minko, T., Poly(propyleneimine) dendrimers as potential siRNA delivery nanocarrier: from structure to function. *Int. J. Nanotechnol.* **2011,** *8* (1-2), 36-52.

23. Nomani, A.; Fouladdel, S.; Haririan, I.; Rahimnia, R.; Ruponen, M.; Gazori, T.; Azizi, E., Poly (amido amine) dendrimer silences the expression of epidermal growth factor receptor and p53 gene in vitro. *Afr. J. Pharm. Pharmacol.* **2012,** *6* (8), 530-537.
24. Patil, M. L.; Zhang, M.; Minko, T., Multifunctional Triblock Nanocarrier (PAMAM-PEG-PLL) for the Efficient Intracellular siRNA Delivery and Gene Silencing. *Acs Nano* **2011,** *5* (3), 1877-1887.
25. Tsai, Y.-J.; Hu, C.-C.; Chu, C.-C.; Toyoko, I., Intrinsically Fluorescent PAMAM Dendrimer as Gene Carrier and Nanoprobe for Nucleic Acids Delivery: Bioimaging and Transfection Study. *Biomacromolecules* **2011,** *12* (12), 4283-4290.
26. Ramsden, J. D.; Cocks, H. C.; Shams, M.; Nijjar, S.; Watkinson, J. C.; Sheppard, M. C.; Ahmed, A.; Eggo, M. C., Tie-2 is expressed on thyroid follicular cells, is increased in colter, and is regulated by thyrotropin through cyclic adenosine 3 ',5 '-monophosphate. *J. Clin. Endocrinol. Metab.* **2001,** *86* (6), 2709-2716.
27. Sato, T. N.; Qin, Y.; Kozak, C. A.; Audus, K. L., Tie-1 and tie-2 define another class of putative receptor tyrosine kinase genes expressed in early embryonic vascular system. *Proc. Natl. Acad. Sci. U. S. A.* **1993,** *90* (20), 9355-9358.
28. Arai, F.; Hirao, A.; Ohmura, M.; Sato, H.; Matsuoka, S.; Takubo, K.; Ito, K.; Koh, G. Y.; Suda, T., Tie2/angiopoietin-1 signaling regulates hematopoietic stem cell quiescence in the bone marrow niche. *Cell* **2004,** *118* (2), 149-161.
29. Aloia, R. C.; Tian, H.; Jensen, F. C., Lipid composition and fluidity of the human immunodeficiency virus envelope and host cell plasma membranes. *Proc. Natl. Acad. Sci. U. S. A.* **1993,** *90* (11), 5181-5185.
30. Cukierman, E.; Pankov, R.; Stevens, D. R.; Yamada, K. M., Taking cell-matrix adhesions to the third dimension. *Science* **2001,** *294* (5547), 1708-1712.
31. Jackson, E. L.; Olive, K. P.; Tuveson, D. A.; Bronson, R.; Crowley, D.; Brown, M.; Jacks, T., The differential effects of mutant p53 alleles on advanced murine lung cancer. *Cancer Res.* **2005,** *65* (22), 10280-10288.
32. Xue, W.; Dahlman, J. E.; Tammela, T.; Khan, O. F.; Sood, S.; Dave, A.; Cai, W.; Chirino, L. M.; Yang, G. R.; Bronson, R.; Crowley, D. G.; Sahay, G.; Schroeder, A.; Langer, R.; Anderson, D. G.; Jacks, T., Small RNA combination therapy for lung cancer. *Proc. Natl. Acad. Sci. U. S. A.* **2014,** *111* (34), E3553-E3561.
33. Maeda, H.; Fang, J.; Inutsuka, T.; Kitamoto, Y., Vascular permeability enhancement in solid tumor: Various factors, mechanisms involved and its implications. *Int. Immunopharmacol.***2003,** *3* (3), 319-328.
34. De Perrot, M.; Sekine, Y.; Fischer, S.; Waddell, T. K.; McRae, K.; Liu, M. Y.; Wigle, D. A.; Keshavjee, S., Interleukin-8 release during early reperfusion predicts graft function in human lung transplantation. *Am. J. Respir. Crit. Care Med.* **2002,** *165* (2), 211-215.
35. Lesniak, A.; Salvati, A.; Santos-Martinez, M. J.; Radomski, M. W.; Dawson, K. A.; Åberg, C., Nanoparticle adhesion to the cell membrane and its effect on nanoparticle uptake efficiency. *J. Am. Chem. Soc.* **2013,** *135* (4), 1438-1444.
36. Wang, Z.; Tiruppathi, C.; Minshall, R. D.; Malik, A. B., Size and dynamics of caveolae studied using nanoparticles in living endothelial cells. *ACS Nano* **2009,** *3* (12), 4110-4116.
37. Whitehead, K. A.; Dorkin, J. R.; Vegas, A. J.; Chang, P. H.; Veiseh, O.; Matthews, J.; Fenton, O. S.; Zhang, Y.; Olejnik, K. T.; Yesilyurt, V.; Chen, D.; Barros, S.; Klebanov, B.; Novobrantseva, T.; Langer, R.; Anderson, D. G., Degradable lipid nanoparticles with predictable in vivo siRNA delivery activity. *Nat. Commun.* **2014,** *5*.
38. Alabi, C. A.; Love, K. T.; Sahay, G.; Yin, H.; Luly, K. M.; Langer, R.; Anderson, D. G., Multiparametric approach for the evaluation of lipid nanoparticles for siRNA delivery. *Proc. Natl. Acad. Sci. U. S. A.* **2013,** *110* (32), 12881-12886.

39. Khan, O. F.; Zaia, E. W.; Yin, H.; Bogorad, R. L.; Pelet, J. M.; Webber, M. J.; Zhuang, I.; Dahlman, J. E.; Langer, R.; Anderson, D. G., Ionizable amphiphilic dendrimer-based nanomaterials with alkyl-chain-substituted amines for tunable siRNA delivery to the liver endothelium in vivo. *Angew. Chem., Int. Ed.* **2014,** *53* (52), 14397-401.
40. DuPage, M.; Dooley, A. L.; Jacks, T., Conditional mouse lung cancer models using adenoviral or lentiviral delivery of Cre recombinase. *Nat. Protoc.* **2009,** *4* (7), 1064-1072.

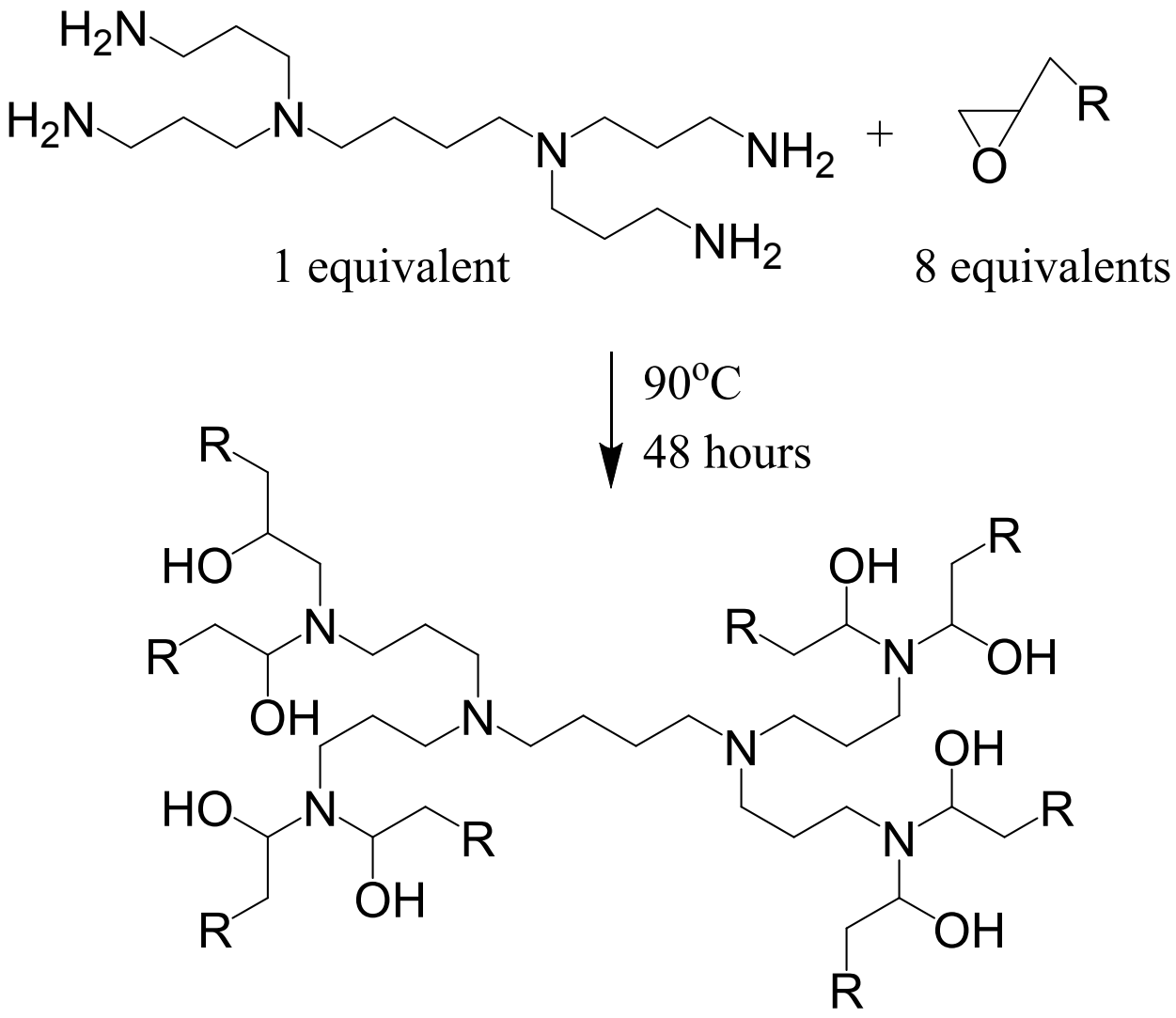

Scheme 1. Example synthesis of lipid-like dendrimer materials. Epoxide-terminated alkyl chains ranging in size from C_{10} to C_{16} were reacted with the free amines in poly(propylenimine) and poly(amido amine) dendrimers of increasing generation size. In this example, a generation 1 poly(propylenimine) is reacted with an epoxide.

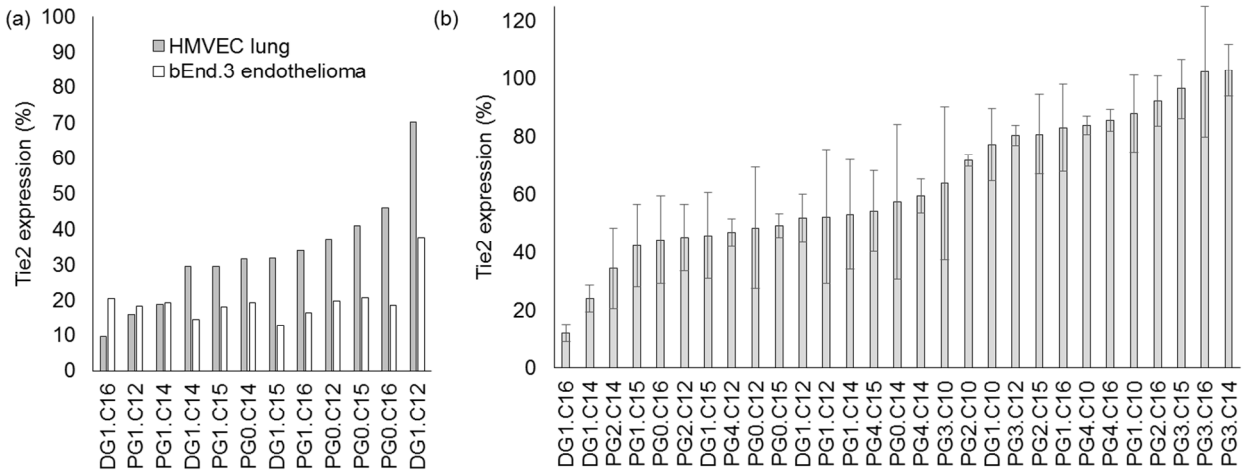

Figure 1. Screening modified dendrimers for siRNA delivery and gene knockdown. Poly(amido amine) and poly(propylenimine) products were denoted as PGx.Cy and DGx.Cy, respectively, where x was the generation number and y the alkyl chain length. (a) Initial low-generation *in vitro* modified dendrimer screen. Primary human microvascular endothelial cells (HMVEC) from the lung and immortalized bEnd.3 endothelial cells from brain endothelioma were treated overnight with modified dendrimer nanoparticles carrying Tie2 siRNA at a 50 nM dose. Values are averages from duplicate experiments and are relative to PBS treated controls. (b) *In vivo* lung screen with modified dendrimer nanoparticles formulated with Tie2 siRNA. Mice were injected with a single 2.5 mg/kg Tie2 siRNA dose and gene expression was quantified after 3 days. The top 3 performing materials were selected for further optimization. Gene expression values are relative to PBS-treated controls. N = 3 and error bars ± S.D.

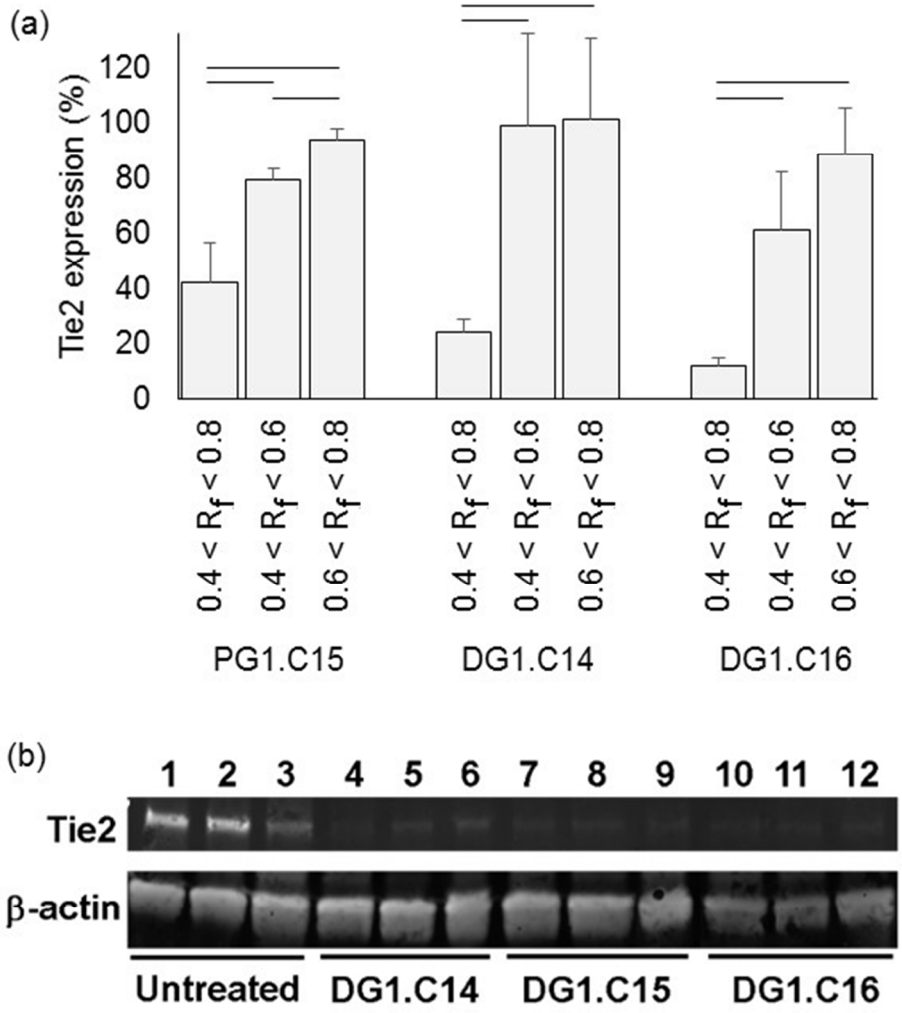

Figure 2. (a) The effect the degree of alkyl chain substitution has on nanoparticle performance. Synergistic effects of modified dendrimer nanoparticles containing a range of alkyl chain substitutions in the lung endothelium. The synthesis of the chemically-modified dendrimers resulted in a mixture of materials with different levels of substitution. The mixture ($0.4 < R_f < 0.8$) was further split into high and low substitution fractions based on R_f values. R_f values between 0.4 and 0.6 had a lower amount of substitution while R_f values between 0.6 and 0.8 had higher amounts of substitution. The *in vivo* efficacy of the different mixtures were compared 2 days after a 2.5 mg/kg Tie2 siRNA nanoparticle dose. The full mixture containing the broadest

range of substitution outperformed the subfractions. Gene expression values are normalized to PBS treated controls. N = 3 and error bars + 1 S.D. Connecting lines indicate $p < 0.009$ (ANOVA with Tukey multiple comparison correction) for comparisons between the gene expression of the mixture and the subfractions. (b) Western blot showing a reduction in Tie2 protein expression in the lung 2 days after a 2.5 mg/kg Tie2 siRNA treatment with DG1-class chemically-modified dendrimers. DG1.C14, DG1.C15 and DG1.C16 all showed excellent protein knockdown. N = 3.

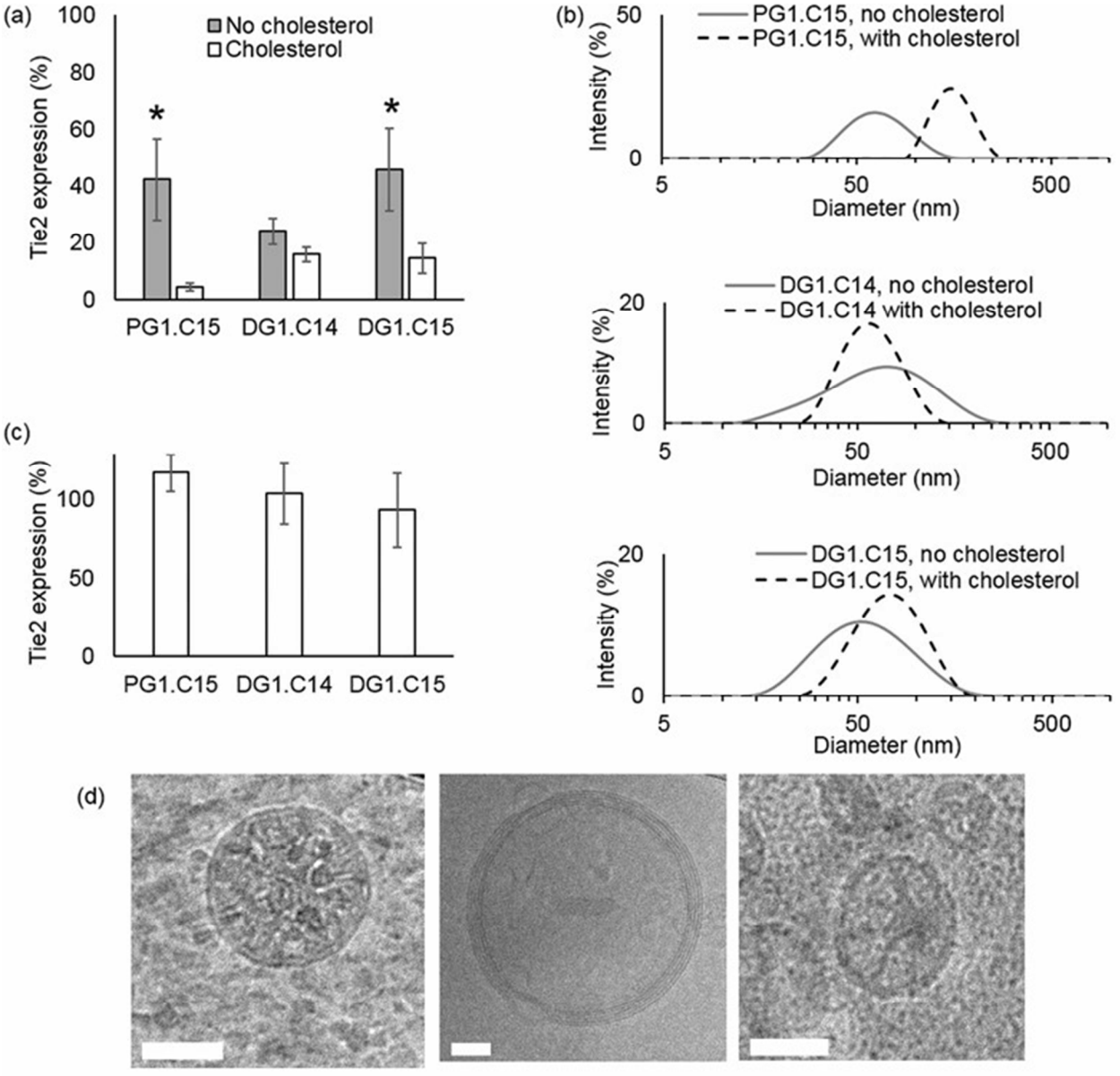

Figure 3. (a) Optimized modified dendrimer formulations. To tune delivery to lung endothelial cells *in vivo*, cholesterol was added as a nanoparticle excipient. The additional excipient improved Tie2 knockdown after a single Tie2 siRNA dose of 2.5 mg/kg. Gene expression values are normalized to PBS treated controls. N = 3 and error bars ± S.D. * = $p < 0.03$ (t-test) in comparison to cholesterol use. (b) Nanoparticle size comparison with and without cholesterol. The polydispersity in nanoparticle size decreased with the addition of cholesterol. For nanoparticles containing C_{15} alkyl chains, the mean nanoparticle diameters also increased with

the addition of cholesterol. (c) Negative controls for optimized modified dendrimer formulations. No Tie2 knockdown was seen when animals were treated with chemically-modified dendrimers carrying non-functional luciferase siRNA. N = 3 and error bars ± S.D. (d) Cryogenic transmission electron microscope images of optimized PG1.C15 (left), DG1.C14 (middle) and DG1.C15 (right) nanoparticles. The dark regions that appear as folds or rings are the internal lamellar structures of the nanoparticles. Scale bars = 50 nm.

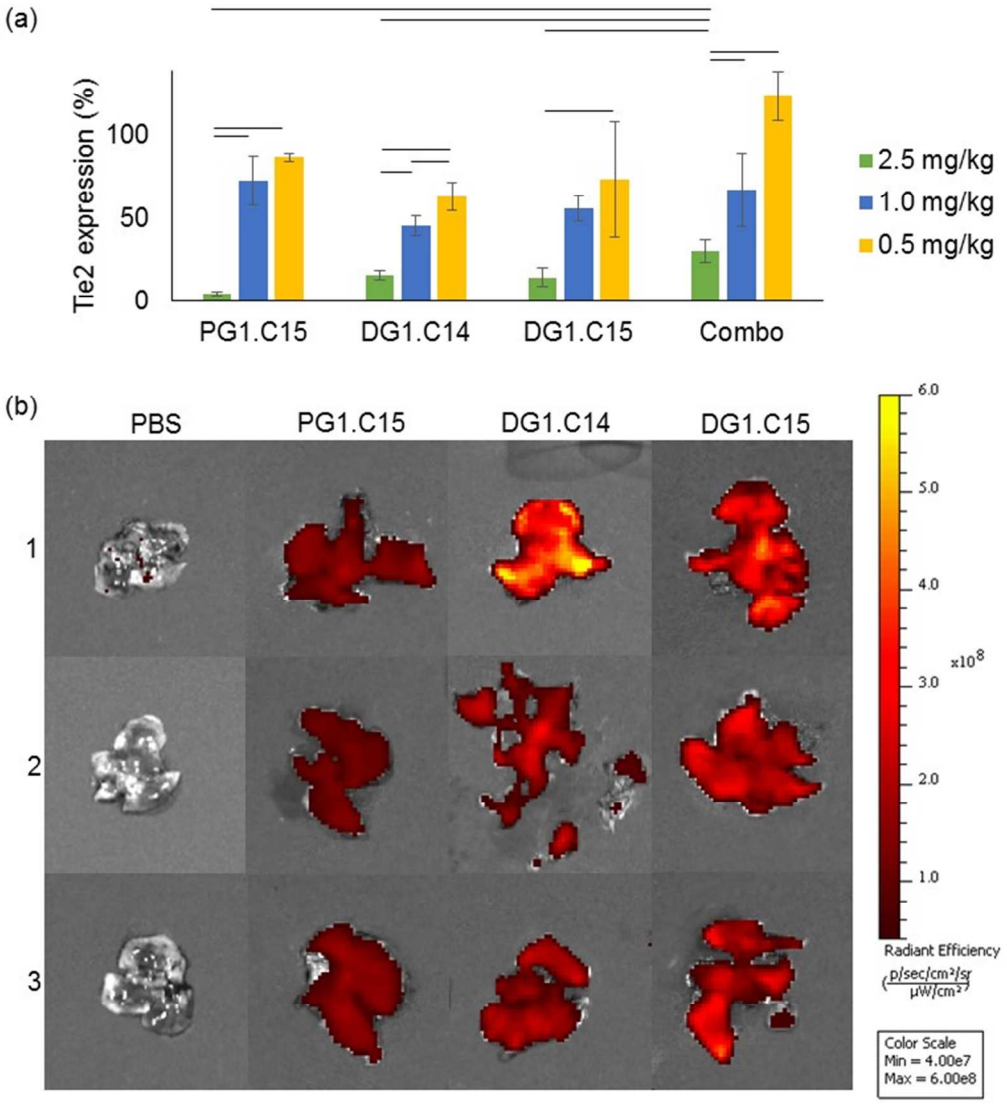

Figure 4. (a) Tie2 siRNA dose response using the top 3 nanoparticles, as well as a mixture of the three. For these dose responses, the optimized, cholesterol-containing formulations were used (refer to Table 2). Gene expression values are normalized to PBS treated controls. N = 3 and error bars ± S.D. Connecting lines indicate $p < 0.05$ by ANOVA with Tukey multiple comparison correction. (b) The relative, qualitative differences in lung fluorescence between PG1.C15, DG1.C14 and DG1.C15 formulated with Cy5.5-tagged siRNA. Modified dendrimer nanoparticles were injected into the tail veins of mice and after 1 hour, lungs were harvested and imaged. Total siRNA dose = 1 mg/kg and n = 3.

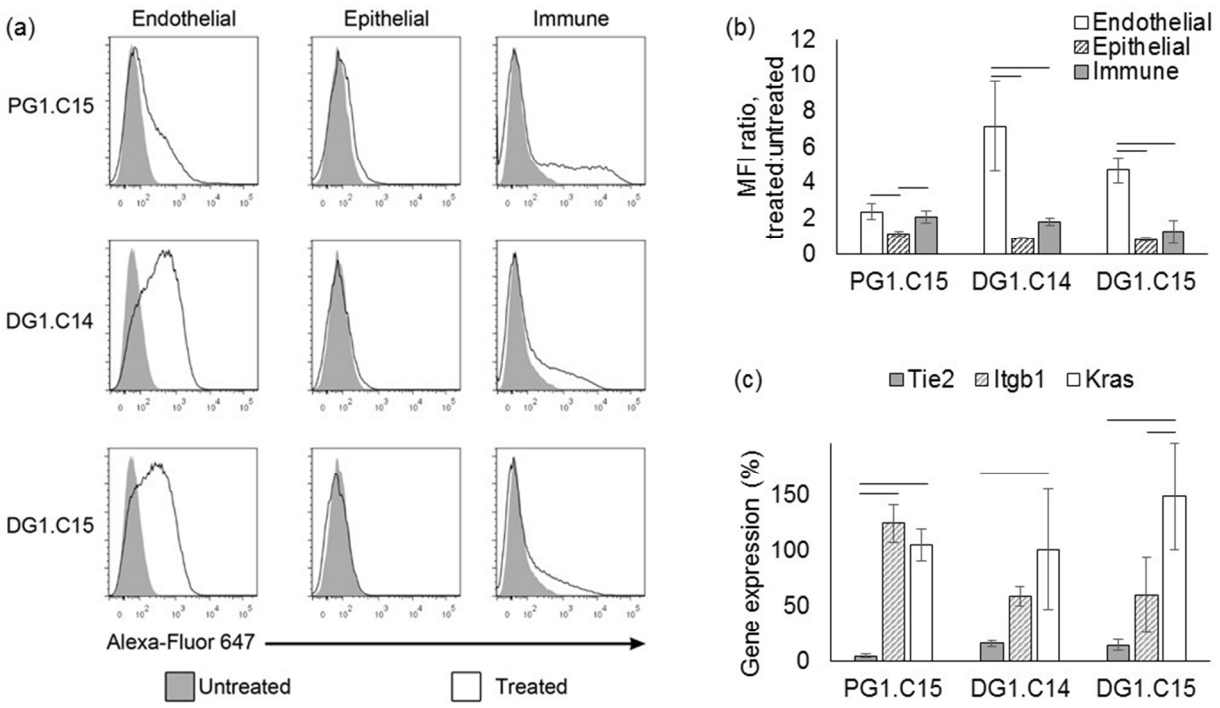

Figure 5. (a) Preferential nanoparticle association and uptake in lung endothelial cells as shown by flow cytometry. Chemically-modified dendrimers were formulated with Alexa-Fluor 647-tagged siRNA and injected into the tail vein of mice. One hour post-injection, lungs were harvested and a single cell suspension was prepared for flow cytometry analysis. Endothelial cells were identified as CD31+, CD45- and EPCAM-, epithelial cells as EPCAM+, CD31- and CD45, and immune cells as CD45+, CD31- and EPCAM-. Grey curves are untreated controls and white are nanoparticle treated. A large peak shift in fluorescent intensity was observed for endothelial cells, which contrasted with the lack of shift in epithelial cells and a modest shift in immune cells. (b) Quantification of nanoparticle association and uptake in terms of the Median Fluorescent Intensity (MFI) for each treatment. Endothelial cells showed a statistically significant increase in nanoparticle association and uptake, as compared to epithelial cells, for all three nanomaterials. DG1-class materials also showed a significant increase in endothelial cell uptake, as compared to immune cells. Connecting lines indicate $p < 0.05$ by ANOVA with

Tukey multiple comparison correction. N = 5 and error bars are ± S.D. (c) To confirm preferential endothelial cell delivery, chemically-modified dendrimers were formulated with siRNA against itbg1 and Kras. Normal mice were dosed with Tie2 or Itgb1 siRNA at 2.5 mg/kg while KP mice with mutated Kras-driven lung tumors were treated with Kras siRNA at a total dose of 4 mg/kg. Unlike Tie2, there was no Itgb1 knockdown in PG1.C15 and modest knockdown in DG1.C14 and DG1.C15. No Kras knockdown was observed for any of the treatments. Gene expression values are normalized to PBS-treated controls. N = 3 for Tie2 experiments and n = 4 for Itgb1 and Kras experiments. Error bars ± S.D. Connecting lines indicate $p < 0.05$ by ANOVA with Tukey multiple comparison correction.

Table 1. Zeta potential and apparent nanoparticle pK_a values of top 4 lead materials prior to optimization.

Modified dendrimer	Zeta potential ± standard deviation (mV)	Apparent nanoparticle pK_a
PG1.C15	-10.7 ± 1.8	5.5
DG1.C14	-10.4 ± 2.6	6.7
DG1.C15	-13.2 ± 2.9	5.5
DG1.C16	-6.7 ± 2.0	5.0

Table 2. Optimized nanoparticle formulations of the top 3 lead materials for delivery to lung endothelial cells.

Modified dendrimer	Modified dendrimer:siRNA mass ratio	Modified dendrimer:cholesterol:1,2-dimyristoyl-sn-glycero-3-phosphoethanolamine-N-mPEG$_{2000}$ mass ratio	
		Cholesterol-free formulation used in initial screens	Optimized cholesterol-containing formulations for enhanced lung endothelium potency
PG1.C15	5:1	92:0:8	97:1:2
DG1.C14	5:1	75:0:25	90:3:7
DG1.C15	5:1	76:0:24	90:3:7

Table of Contents Graphic

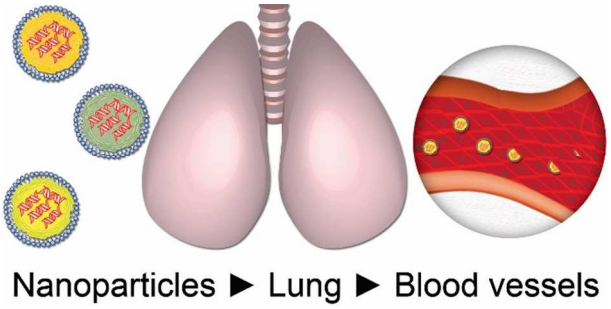

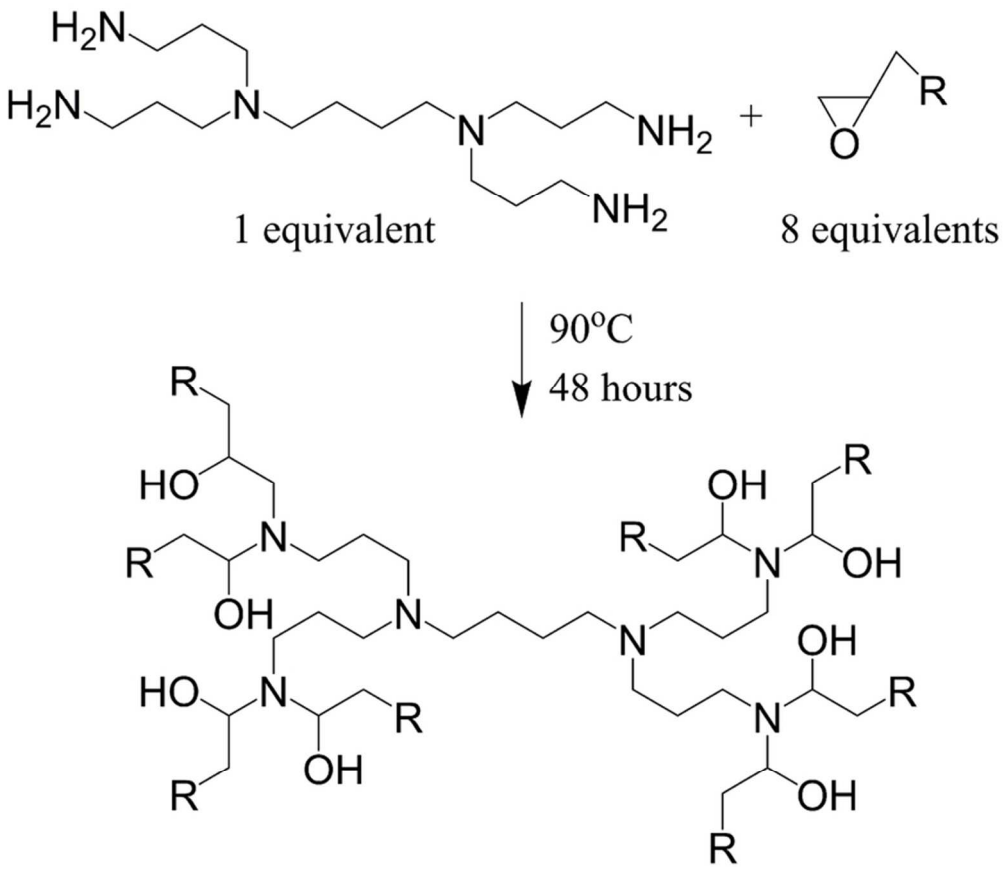

Example synthesis of lipid-like dendrimer materials. Epoxide-terminated alkyl chains ranging in size from C_{10} to C_{16} were reacted with the free amines in poly(propylenimine) and poly(amido amine) dendrimers of increasing generation size. In this example, a generation 1 poly(propylenimine) is reacted with an epoxide.
72x62mm (300 x 300 DPI)

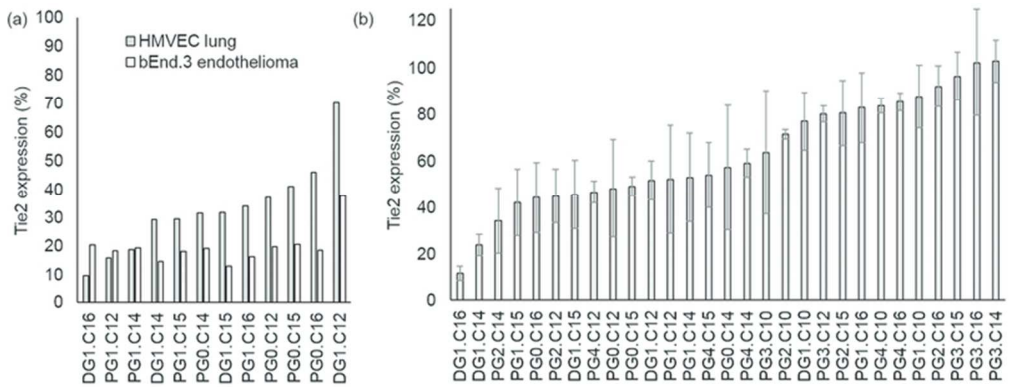

Screening modified dendrimers for siRNA delivery and gene knockdown. Poly(amido amine) and poly(propylenimine) products were denoted as PGx.Cy and DGx.Cy, respectively, where x was the generation number and y the alkyl chain length. (a) Initial low-generation in vitro modified dendrimer screen. Primary human microvascular endothelial cells (HMVEC) from the lung and immortalized bEnd.3 endothelial cells from brain endothelioma were treated overnight with modified dendrimer nanoparticles carrying Tie2 siRNA at a 50 nM dose. Values are averages from duplicate experiments and are relative to PBS treated controls. (b) In vivo lung screen with modified dendrimer nanoparticles formulated with Tie2 siRNA. Mice were injected with a single 2.5 mg/kg Tie2 siRNA dose and gene expression was quantified after 3 days. The top 3 performing materials were selected for further optimization. Gene expression values are relative to PBS-treated controls. N = 3 and error bars ± S.D.
67x25mm (300 x 300 DPI)

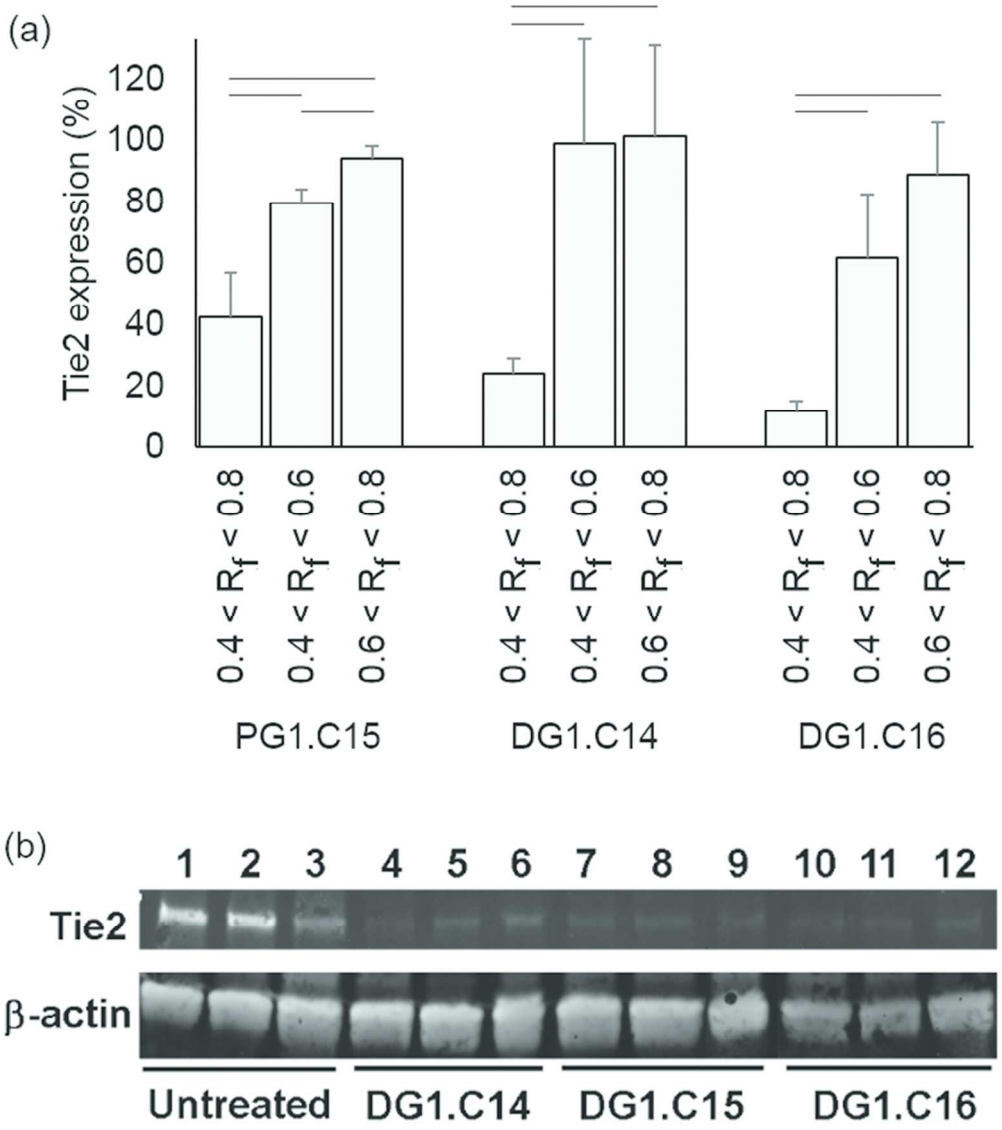

(a) The effect the degree of alkyl chain substitution has on nanoparticle performance. Synergistic effects of modified dendrimer nanoparticles containing a range of alkyl chain substitutions in the lung endothelium. The synthesis of the chemically-modified dendrimers resulted in a mixture of materials with different levels of substitution. The mixture ($0.4 < R_f < 0.8$) was further split into high and low substitution fractions based on R_f values. R_f values between 0.4 and 0.6 had a lower amount of substitution while R_f values between 0.6 and 0.8 had higher amounts of substitution. The in vivo efficacy of the different mixtures were compared 2 days after a 2.5 mg/kg Tie2 siRNA nanoparticle dose. The full mixture containing the broadest range of substitution outperformed the subfractions. Gene expression values are normalized to PBS treated controls. N = 3 and error bars + 1 S.D. Connecting lines indicate $p < 0.009$ (ANOVA with Tukey multiple comparison correction) for comparisons between the gene expression of the mixture and the subfractions. (b) Western blot showing a reduction in Tie2 protein expression in the lung 2 days after a 2.5 mg/kg Tie2 siRNA treatment with DG1-class chemically-modified dendrimers. DG1.C14, DG1.C15 and DG1.C16 all showed excellent protein knockdown. N = 3.
94x107mm (300 x 300 DPI)

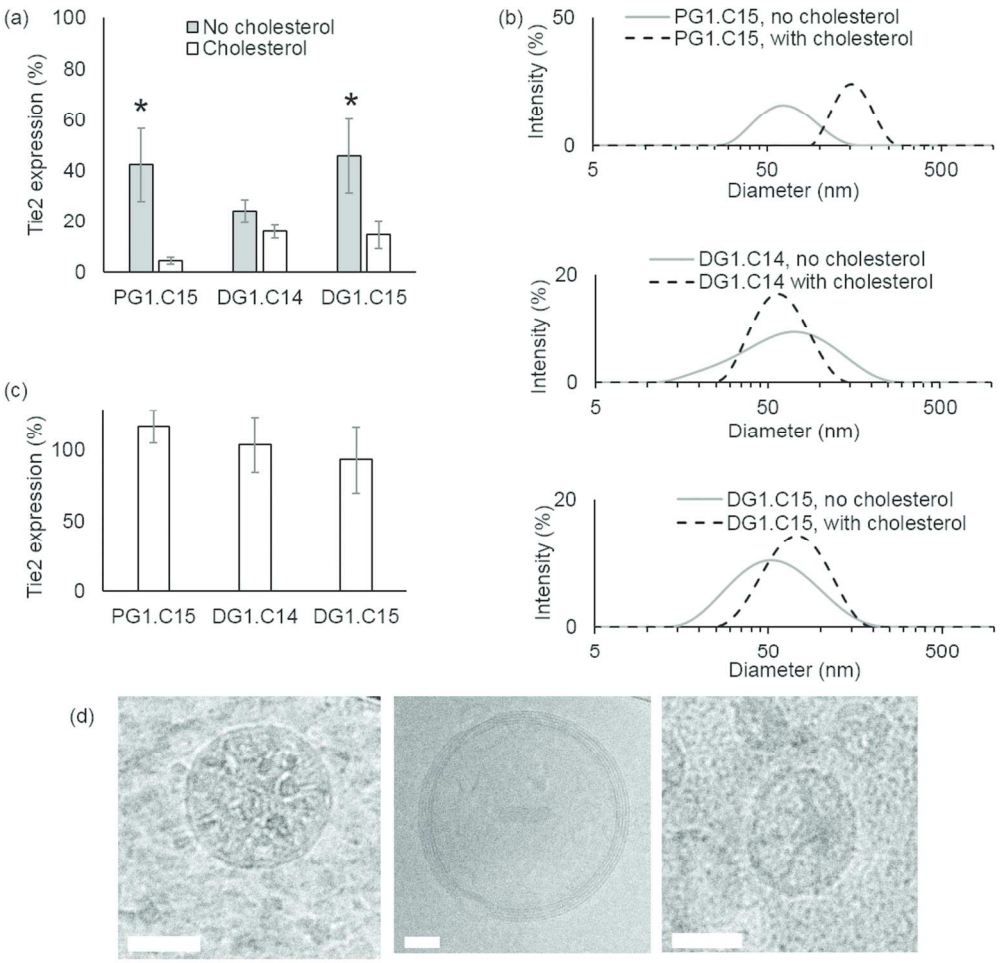

(a) Optimized modified dendrimer formulations. To tune delivery to lung endothelial cells in vivo, cholesterol was added as a nanoparticle excipient. The additional excipient improved Tie2 knockdown after a single Tie2 siRNA dose of 2.5 mg/kg. Gene expression values are normalized to PBS treated controls. N = 3 and error bars ± S.D. * = $p < 0.03$ (t-test) in comparison to cholesterol use. (b) Nanoparticle size comparison with and without cholesterol. The polydispersity in nanoparticle size decreased with the addition of cholesterol. For nanoparticles containing C15 alkyl chains, the mean nanoparticle diameters also increased with the addition of cholesterol. (c) Negative controls for optimized modified dendrimer formulations. No Tie2 knockdown was seen when animals were treated with chemically-modified dendrimers carrying non-functional luciferase siRNA. N = 3 and error bars ± S.D. (d) Cryogenic transmission electron microscope images of optimized PG1.C15 (left), DG1.C14 (middle) and DG1.C15 (right) nanoparticles. The dark regions that appear as folds or rings are the internal lamellar structures of the nanoparticles. Scale bars = 50 nm.
170x163mm (300 x 300 DPI)

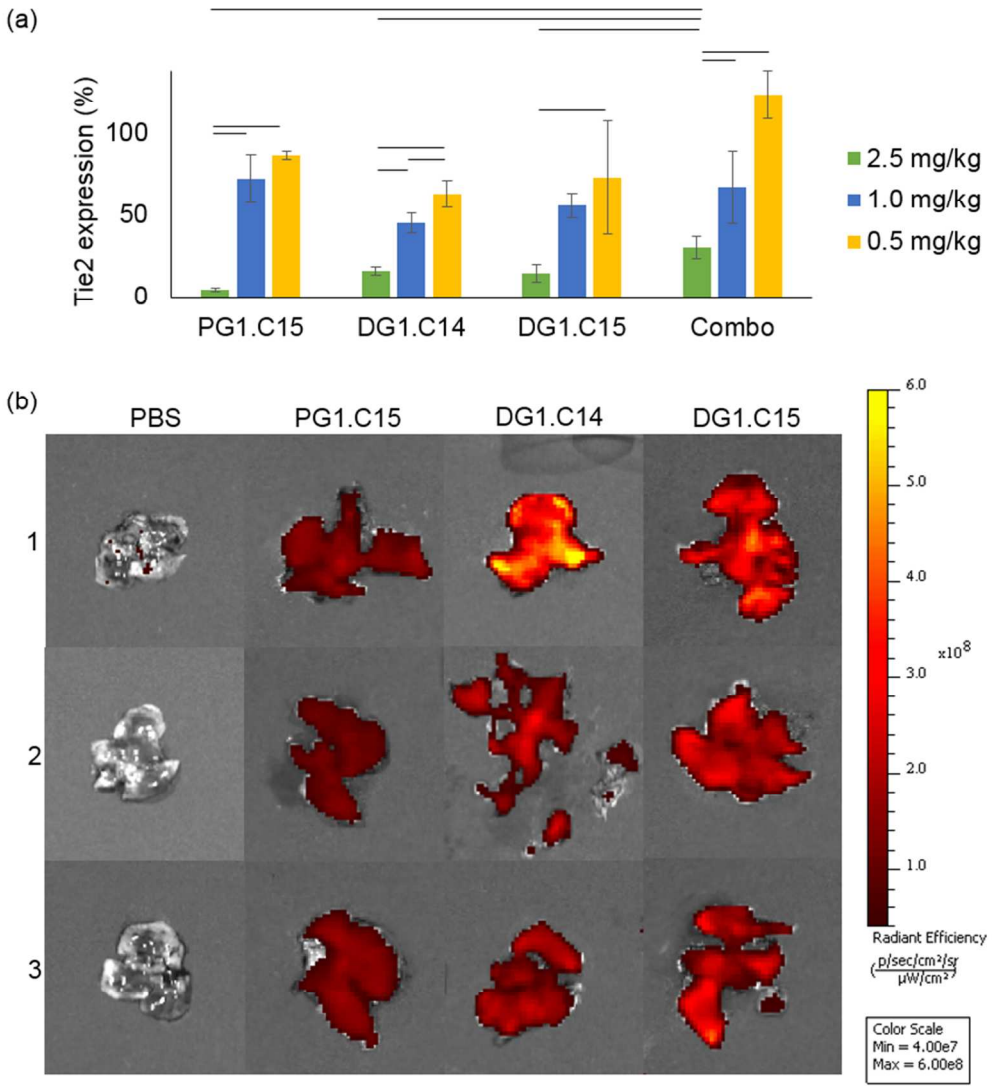

(a) Tie2 siRNA dose response using the top 3 nanoparticles, as well as a mixture of the three. For these dose responses, the optimized, cholesterol-containing formulations were used (refer to Table 2). Gene expression values are normalized to PBS treated controls. N = 3 and error bars ± S.D. Connecting lines indicate $p < 0.05$ by ANOVA with Tukey multiple comparison correction. (b) The relative, qualitative differences in lung fluorescence between PG1.C15, DG1.C14 and DG1.C15 formulated with Cy5.5-tagged siRNA. Modified dendrimer nanoparticles were injected into the tail veins of mice and after 1 hour, lungs were harvested and imaged. Total siRNA dose = 1 mg/kg and n = 3.
192x208mm (300 x 300 DPI)

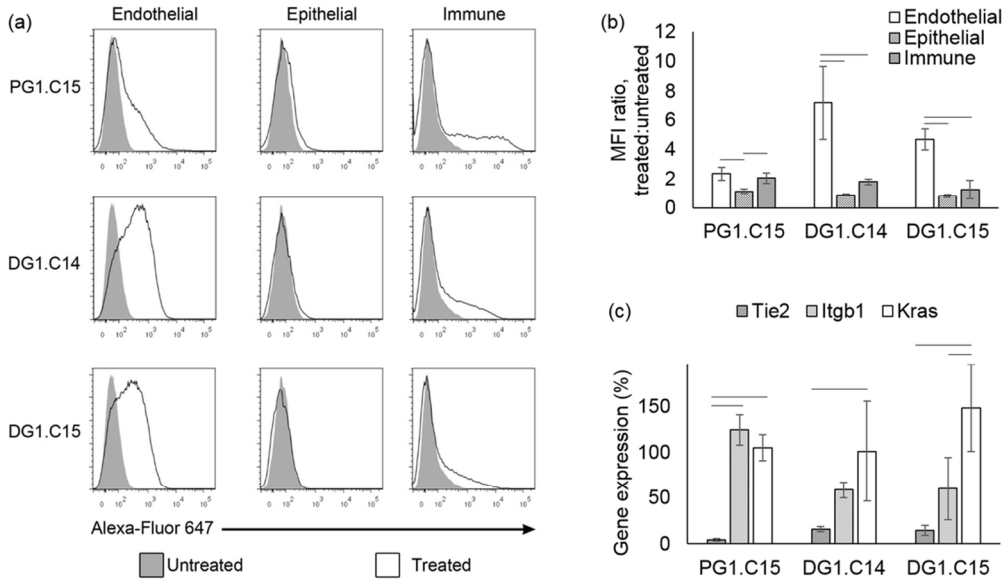

(a) Preferential nanoparticle association and uptake in lung endothelial cells as shown by flow cytometry. Chemically-modified dendrimers were formulated with Alexa-Fluor 647-tagged siRNA and injected into the tail vein of mice. One hour post-injection, lungs were harvested and a single cell suspension was prepared for flow cytometry analysis. Endothelial cells were identified as CD31+, CD45- and EPCAM-, epithelial cells as EPCAM+, CD31- and CD45, and immune cells as CD45+, CD31- and EPCAM-. Grey curves are untreated controls and white are nanoparticle treated. A large peak shift in fluorescent intensity was observed for endothelial cells, which contrasted with the lack of shift in epithelial cells and a modest shift in immune cells. (b) Quantification of nanoparticle association and uptake in terms of the Median Fluorescent Intensity (MFI) for each treatment. Endothelial cells showed a statistically significant increase in nanoparticle association and uptake, as compared to epithelial cells, for all three nanomaterials. DG1-class materials also showed a significant increase in endothelial cell uptake, as compared to immune cells. Connecting lines indicate $p < 0.05$ by ANOVA with Tukey multiple comparison correction. N = 5 and error bars are ± S.D. (c) To confirm preferential endothelial cell delivery, chemically-modified dendrimers were formulated with siRNA against itbg1 and Kras. Normal mice were dosed with Tie2 or Itgb1 siRNA at 2.5 mg/kg while KP mice with mutated Kras-driven lung tumors were treated with Kras siRNA at a total dose of 4 mg/kg. Unlike Tie2, there was no Itgb1 knockdown in PG1.C15 and modest knockdown in DG1.C14 and DG1.C15. No Kras knockdown was observed for any of the treatments. Gene expression values are normalized to PBS-treated controls. N = 3 for Tie2 experiments and n = 4 for Itgb1 and Kras experiments. Error bars ± S.D. Connecting lines indicate $p < 0.05$ by ANOVA with Tukey multiple comparison correction.

102x59mm (300 x 300 DPI)

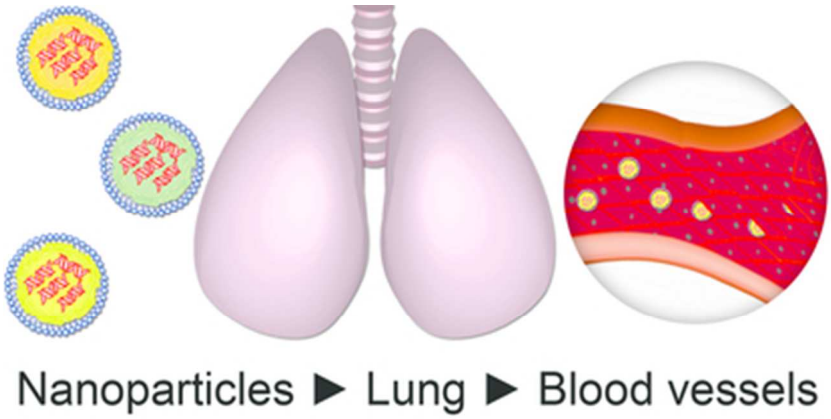

34x17mm (300 x 300 DPI)